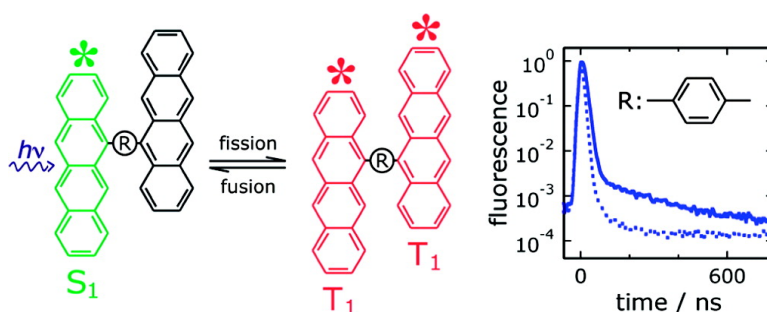


Exciton Fission and Fusion in Bis(tetracene) Molecules with Different Covalent Linker Structures

Astrid M. Müller, Yuri S. Avlasevich, Wolfgang W. Schoeller, Klaus Müllen, and Christopher J. Bardeen

J. Am. Chem. Soc., **2007**, 129 (46), 14240-14250 • DOI: 10.1021/ja073173y • Publication Date (Web): 25 October 2007

Downloaded from <http://pubs.acs.org> on February 13, 2009



More About This Article

Additional resources and features associated with this article are available within the HTML version:

- Supporting Information
- Links to the 2 articles that cite this article, as of the time of this article download
- Access to high resolution figures
- Links to articles and content related to this article
- Copyright permission to reproduce figures and/or text from this article

[View the Full Text HTML](#)

Exciton Fission and Fusion in Bis(tetracene) Molecules with Different Covalent Linker Structures

Astrid M. Müller,[†] Yuri S. Avlasevich,[‡] Wolfgang W. Schoeller,^{†,§} Klaus Müllen,[‡] and Christopher J. Bardeen^{*†}

Contribution from the Department of Chemistry, University of California, Riverside, California 92521, Max Planck Institute for Polymer Research, Ackermannweg 10, D-55128 Mainz, Germany, and Department of Chemistry, University of Bielefeld, D-33503 Bielefeld, Germany

Received May 4, 2007; E-mail: christopher.bardeen@ucr.edu

Abstract: Bichromophoric molecules can support two spatially separated excited states simultaneously and thus provide novel pathways for electronic state relaxation. Exciton fission, where absorption of a single photon leads to two triplet states, is a potentially useful example of such a pathway. In this paper, a detailed study of exciton fission in three novel phenylene-linked bis(tetracene) molecules is presented. Their spectroscopy is analyzed in terms of a three-state kinetic model in which the singlet excited state can fission into a triplet pair state, which in turn undergoes recombination on a time scale longer than the molecule's radiative lifetime. This model allows us to fit both the prompt and delayed fluorescence decay data quantitatively. The para-phenylene linked bis(tetracene) molecules 1,4-bis(tetracene-5-yl)benzene (**1**) and 4,4'-bis(tetracene-5-yl)biphenylene (**2**) show intramolecular exciton fission with yields of ~3%, whereas no delayed fluorescence is observed for tetracene or the meta-linked molecule 1,3-bis(tetracene-5-yl)benzene **3**. Analysis of the temperature-dependent fluorescence dynamics yields activation energies for fission of (10.0 ± 0.6) kJ/mol for **1** and (4.1 ± 0.5) kJ/mol for **2**, with Arrhenius prefactors of (1.48 ± 0.04) × 10⁸ s⁻¹ for **1** and (1.72 ± 0.02) × 10⁷ s⁻¹ for **2**. The observed trends in activation energies are reproduced by *ab initio* calculations of the independently optimized singlet and triplet energies. The calculations indicate that electronic coupling between the two tetracene units is primarily through-bond, allowing differences in fission rates to be qualitatively explained in terms of the linker structure as well. Our results show that it is important to consider the effects of the linker structure on both energy relaxation and electronic coupling in bichromophoric molecules. This study provides insight into the structural and energetic factors that should be taken into account in the design of exciton fission molecules for possible solar cell applications.

Introduction

The dual pressures of global warming and dwindling fossil fuel supplies are forcing society to search for alternative energy sources. One of the most promising avenues for alternative energy production is solar energy conversion, usually in the form of photovoltaic conversion of photons into electricity. But although solar photovoltaics provide an environmentally benign, potentially unlimited source of electricity, their high cost and limited efficiencies prevent widespread adoption.¹ To drive down the cost of photovoltaic materials, there is currently intense interest in using organic semiconductors instead of the current generation of inorganic materials. To increase solar cell efficiency, both new types of materials and new strategies for the photon → electron–hole pair conversion process are being studied. In terms of the latter effort, there is strong interest in taking advantage of the phenomenon of multiple exciton

generation (MEG) to increase the yield of excitations per absorbed photon. In MEG, a single photon produces multiple excitons that, in principle, can then be turned into multiple electron–hole pairs. Two types of MEG have been observed. The first type is a singlet → singlet splitting of a high energy state S* into two or more low-energy excited states S₁:



Originally proposed as a strategy to increase solar cell efficiencies,^{2,3} this process was first observed in PbSe nanocrystals⁴ and has since been confirmed in a variety of other semiconductor nanocrystals.^{5–7} MEG is theoretically capable of increasing the

[†] University of California.

[‡] Max Planck Institute for Polymer Research.

[§] University of Bielefeld.

(1) D.O.E. Basic energy needs for solar energy utilization. Presented at B.E.S. Workshop, 2005.

(2) Nozik, A. J. *Ann. Rev. Phys. Chem.* **2001**, 52, 193–231.

(3) Nozik, A. J. *Physica E* **2002**, 14, 115–120.

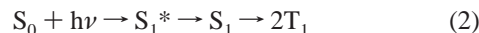
(4) Schaller, R. D.; Klimov, V. I. *Phys. Rev. Lett.* **2004**, 92, 186601/1–186601/4.

(5) Schaller, R. D.; Petruska, M. A.; Klimov, V. I. *Appl. Phys. Lett.* **2005**, 87, 253102/1–253102/3.

(6) Ellingson, R. J.; Beard, M. C.; Johnson, J. C.; Yu, P.; Micic, O. I.; Nozik, A. J.; Shabaev, A.; Efros, A. L. *Nano Lett.* **2005**, 5, 865–871.

(7) Murphy, J. E.; Beard, M. C.; Norman, A. G.; Ahrenkiel, S. P.; Johnson, J. C.; Yu, P.; Micic, O. I.; Ellingson, R. J.; Nozik, A. J. *J. Am. Chem. Soc.* **2006**, 128, 3241–3247.

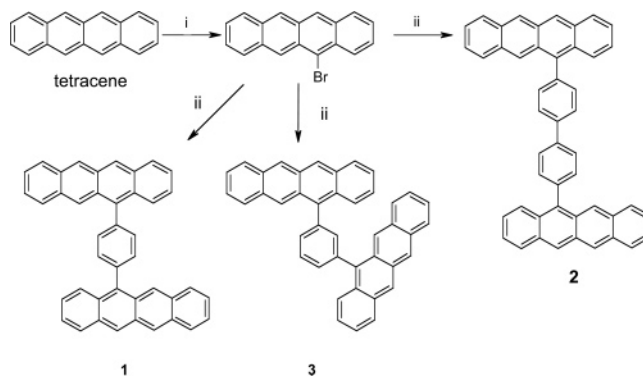
efficiency of a functioning solar cell by a factor of 1.5–2.0, although there is some disagreement as to the maximum enhancement possible.^{8,9} A second variant of the MEG phenomenon is the singlet → triplet channel, where the relaxed excited singlet state S_1 splits into a pair of triplets T_1 .



This reaction has been known in organic solids for several decades^{10,11} and is commonly called “exciton fission”. The inverse of this process, exciton fusion, is also of interest to enhance the photovoltaic response of organic materials.¹² Recent theoretical work has shown that exciton fission is energetically feasible in several broad classes of organic compounds.¹³ Like reaction 1, exciton fission is spin-allowed but with two additional advantages. First, it can occur from the relaxed singlet state, so there is no competition from other rapid intramolecular processes like vibrational relaxation. Second, exciton fission occurs without the requirement for quantum confinement. Thus, the two newly produced triplets are able to diffuse away from each other into the bulk solid, which alleviates the self-annihilation problem commonly seen in the inorganic nanocrystal systems.¹⁴ Given these potential advantages, it is of interest to gain a better understanding of the photophysical dynamics that underlie this process, so that its potential to increase the efficiency of organic solar cells can be evaluated.

The phenomenon of exciton fission has been proposed to explain the anomalously low fluorescence yields in crystalline tetracene,^{15,16} and tetracene remains the most extensively studied fission system. Unfortunately, crystalline tetracene is also a very complicated material with delocalized singlet exciton states and many types of defect states.^{17,18} A much simpler system consists of two tetracene molecules connected together via a covalent linker. This type of covalent assembly is the smallest possible fission system and provides a simple model which can be used to test our qualitative ideas about exciton fission. Varying the chemical nature of the covalent linker provides a way to modulate the electronic coupling between the tetracene moieties and possibly control the fission rate. Such molecules could potentially be used as photosensitizers in hybrid solar cells, where the two excited triplet states rapidly inject electrons into a semiconductor substrate.^{13,19} In Scheme 1, we show three such bis(tetracene) molecules that we have synthesized, along with tetracene itself. In an earlier letter, we made a preliminary report of the room-temperature dynamics of 1,4-bis(tetracene-5-yl)benzene (**1**).²⁰ In this paper, we report a more complete study of the photophysical properties of this family of linked tet-

Scheme 1. Synthesis of 1,4-Bis(tetracene-5-yl)benzene (**1**), 4,4'-bis(tetracene-5-yl)biphenylene (**2**), and 1,3-bis(tetracene-5-yl)benzene (**3**), Starting from Monomeric Tetracene^a



^a Reagents, conditions, and yields: (i) NBS (1 equiv), DMF, CHCl_3 , 60 °C, 3 h, 90%; (ii) arylene diboronic acid (0.5 equiv), $\text{Pd}_2(\text{dba})_3$, DPEPHos, 2 M K_2CO_3 aq, EtOH, toluene, 95 °C, 24 h, 67% (**1**), 58% (**2**), and 42% (**3**).

racenes. In addition to measuring the absorption and fluorescence spectra and prompt fluorescence decays, we also characterize the dynamics of the delayed singlet fluorescence. Intramolecular delayed fluorescence, occurring on a time scale much longer than the singlet radiative lifetime, is a signature of triplet–triplet recombination.²¹ The presence of two triplets within an isolated molecule is the direct result of the fission reaction and thus delayed fluorescence provides a sensitive way to monitor the fission process. Temperature-dependent rate measurements yield information about the activation energies and Arrhenius prefactors for both the forward fission and reverse fusion reactions. *Ab initio* calculations are used to explore the molecular conformations of the dimers, as well as the dependence of the energy level spacing and electronic coupling on linker structure. Our results lead to some general conclusions about how the linker structure can affect the fission reaction, highlighting complexities present even in these relatively simple molecules. Possible extensions of the work, as well as a comparison of our results to previous studies of fission in the crystalline solid, are discussed as well.

Experimental

General. ¹H NMR and ¹³C NMR spectra were recorded in deuterated solvents on Bruker DPX250 and DRX500 spectrometers, using TMS as the internal standard. Infrared spectra were obtained on a Nicolet 320 FT-IR spectrometer. FD mass spectra were obtained on a VG Instruments ZAB 2-SE-FPD. Elemental analyses were performed on a Foss Heraeus Vario EL in the Institute for Organic Chemistry at the University of Mainz. All starting materials were purchased from Aldrich, Acros, or ABCR and used as received.

5-Bromotetracene. A solution of NBS (354 mg, 2 mmol) in dry DMF (40 mL) was added during 1 h into a stirred at 60 °C solution of tetracene (456 mg, 2 mmol) in chloroform (200 mL). The resulting solution was stirred at 60 °C for 3 h. After cooling to room temperature, the reaction mixture was washed with water (2 × 200 mL) and then chloroform was evaporated *in vacuo*. The residue was diluted with water (200 mL), and the precipitate was filtered and dried, giving an orange powder. For analytical purposes, it was purified by column chromatography on silica gel using dichloromethane as eluent. Yield: 552

- (8) Schaller, R. D.; Sykora, M.; Pietryga, J. M.; Klimov, V. I. *Nano Lett.* **2006**, *6*, 424–429.
 (9) Hanna, M. C.; Nozik, A. J. *J. Appl. Phys.* **2006**, *100*, 074510/1–074510/8.
 (10) Singh, S.; Jones, W. J.; Siebrand, W.; Stoicheff, B. P.; Schneider, W. G. *J. Chem. Phys.* **1965**, *42*, 330–342.
 (11) Pope, M.; Swenberg, C. E. *Electronic processes in organic crystals and polymers*, 2nd ed.; Oxford: New York, 1999.
 (12) Balushev, S.; Miteva, T.; Yakutkin, V.; Nelles, G.; Yasuda, A.; Wegner, G. *Phys. Rev. Lett.* **2006**, *97*, 14903/1–14903/4.
 (13) Paci, I.; Johnson, J. C.; Chen, X.; Rana, G.; Popovic, D.; David, D. E.; Nozik, A. J.; Ratner, M. A.; Michl, J. *J. Am. Chem. Soc.* **2006**, *128*, 16546–16553.
 (14) Klimov, V. I. *J. Phys. Chem. B* **2006**, *110*, 16827–16845.
 (15) Swenberg, C. E.; Stacy, W. T. *Chem. Phys. Lett.* **1968**, *2*, 327–328.
 (16) Geacintov, N.; Pope, M.; Vogel, F. *Phys. Rev. Lett.* **1969**, *22*, 593–596.
 (17) Lim, S.-H.; Bjorklund, T. G.; Spano, F. C.; Bardeen, C. J. *Phys. Rev. Lett.* **2004**, *92*, 107402/1–107402/4.
 (18) Piryatinskii, Y. P.; Kurik, M. V. *Mol. Mat.* **1992**, *1*, 43–64.
 (19) Anderson, N. A.; Lian, T. *Ann. Rev. Phys. Chem.* **2005**, *56*, 491–519.

- (20) Müller, A. M.; Avlasevich, Y. S.; Müllen, K.; Bardeen, C. J. *Chem. Phys. Lett.* **2006**, *421*, 518–522.
 (21) Birks, J. B. *Photophysics of aromatic molecules*; Wiley-Interscience: London, 1970.

mg (90%). ¹H NMR (500 MHz, C₂D₂Cl₄, 25 °C): δ = 9.03 (s, 1H), 8.59 (s, 1H), 8.58 (s, 1H), 8.38 (d, ³J=8.5 Hz, 1H), 8.01 (d, ³J=7.4 Hz, 1H), 7.90–7.94 (m, 2H), 7.36–7.48 (m, 4H) ppm; ¹³C NMR (125 MHz, C₂D₂Cl₄, 25 °C): 132.63, 131.86, 131.61, 130.53, 130.39, 129.15, 129.07, 129.02, 128.59, 128.19, 127.79, 127.74, 127.51, 126.67, 126.59, 126.46, 126.35, 125.66 ppm; IR (KBr): ν = 1655, 1558, 1458, 1382, 1311, 1270, 944, 876, 732, 676 cm⁻¹; MS (FD): *m/z* (rel. int.) 308.3 (100%), M⁺; Anal. Calcd for C₁₈H₁₁Br: C, 70.38; H, 3.61. Found: C, 70.19; H, 3.47.

Typical Procedure for the Suzuki Coupling of 5-Bromotetracene with Arylene Diboronic Acids. 5-Bromotetracene (308 mg, 1 mmol) and arylene diboronic acid (0.5 mmol) were dissolved in the mixture of toluene (24 mL) and ethanol (2 mL) in a 50 mL Schlenk flask and flushed with argon. After stirring at 80 °C for 20 min, Pd₂(dba)₃ (tris-(dibenzylideneacetone)dipalladium (0)), 25 mg, 13 μmol), DPEPHos (bis(2-diphenylphosphino)phenyl)ether, 50 mg, 0.1 mmol), and aqueous 2 M K₂CO₃ (4 mL) were added to the solution. The reaction mixture was stirred at 95 °C for 24 h under argon. After cooling, the resulting mixture was washed with water and extracted with toluene. The combined organic extracts were evaporated *in vacuo* and purified by column chromatography on silica gel using petrol ether/dichloromethane, 3:1 as eluent.

1,4-Bis(5-tetraceny)benzene (1). Yield: 178 mg (67%). ¹H NMR (250 MHz, CD₂Cl₂, 25 °C): δ = 8.82 (s, 2H), 8.79 (s, 2H), 8.66 (s, 2H), 8.36 (dd, ³J=7.6 Hz 2H), 8.13–7.98 (m, 6H), 7.80 (d, ³J = 7.8 Hz 2H), 7.55–7.38 (m, 10H) ppm; ¹³C NMR (125 MHz, CD₂Cl₂, 25 °C): 134.6, 132.5, 132.1, 130.8, 130.5, 129.8, 129.6, 129.3, 129.1, 129.0, 128.9, 128.7, 128.6, 128.4, 127.6, 127.3, 126.9, 126.6, 125.8, 125.6, 125.4 ppm; IR (KBr): ν = 3442, 3043, 2922, 2852, 2366, 1629, 895, 743 cm⁻¹; MS (FD): *m/z* (rel. int.) 530.4 (100%), M⁺; Anal. Calcd for C₄₂H₂₆: C, 95.06; H, 4.94. Found: C, 95.17; H, 4.83.

4,4'-Bis(5-tetraceny)-1,1'-biphenylene (2). Yield: 176 mg (58%). ¹H NMR (250 MHz, CD₂Cl₂, 25 °C): δ = 8.73 (s, 2H), 8.69 (s, 2H), 8.38 (s, 2H), 8.04 (d, ³J = 7.8 Hz, 4H), 8.01 (d, ³J = 7.0 Hz, 2H), 7.97 (d, ³J = 8.2 Hz, 2H), 7.80 (d, ³J = 8.1 Hz, 2H), 7.73 (d, ³J=8.7 Hz, 2H), 7.62 (d, ³J = 7.8 Hz, 4H), 7.24–7.39 (m, 8H) ppm; ¹³C NMR (125 MHz, CD₂Cl₂, 25 °C): 140.52, 138.67, 137.05, 132.58, 132.00, 131.81, 131.74, 130.55, 130.23, 129.09, 128.95, 128.51, 128.35, 127.65, 127.49, 127.21, 126.89, 126.00, 125.86, 125.74, 125.63, 125.39 ppm; IR (KBr): ν = 3440, 3040, 2920, 2850, 2360, 1629, 895, 742 cm⁻¹; MS (FD): *m/z* (rel. int.) 608.2 (100%), M⁺; Anal. Calcd for C₄₈H₃₀: C, 95.02; H, 4.98. Found: C, 95.13; H, 4.87.

1,3-Bis(5-tetraceny)benzene (3). Yield: 111 mg (42%). ¹H NMR (250 MHz, CD₂Cl₂, 25 °C): δ = 8.77 (s, 2H), 8.73 (s, 2H), 8.67 (s, 1H), 8.61 (s, 2H), 7.93–8.08 (m, 8H), 7.77 (d, ³J=7.4 Hz, 2H), 7.68 (br.s., 1H), 7.39–7.46 (m, 8H) ppm; ¹³C NMR (125 MHz, CD₂Cl₂, 25 °C) 139.50, 136.88, 135.01, 134.80, 131.81, 131.62, 131.54, 131.19, 131.16, 130.36, 130.06, 129.16, 128.98, 128.88, 128.84, 128.27, 127.16, 127.07, 126.81, 125.93, 125.88, 125.75, 125.59, 125.26 ppm; IR (KBr): ν = 3440, 3040, 2920, 2852, 2360, 1629, 895, 743 cm⁻¹; MS (FD): *m/z* (rel. int.) 531.2 (100%), M⁺; Anal. Calcd for C₄₂H₂₆: C, 95.06; H, 4.94. Found: C, 95.13; H, 4.86.

Photophysics. Tetracene was obtained from TCI, benzene, toluene, and DMF (all spectroscopic grade) were obtained from EM Science, and isopentane (spectroscopic grade) was obtained from Aldrich. All samples were measured in solution in 1 cm path length quartz cuvettes. For temperature-dependent measurements, a 1 cm × 1 cm quartz cuvette filled with degassed solution (solvent mixture: 3 mL toluene, 3 mL isopentane, 2 mL DMF) and tightly closed with a neoprene stopper was placed in a home-built aluminum cuvette mount in a cryostat (Janis ST-100) with a temperature controller (LakeShore 321). The cryostat was evacuated and cooled down to 175 K, using liquid nitrogen as the cryogen, or heated to 325 K. With this setup, the solvent mixtures remained liquid at all temperatures. The samples were degassed by bubbling argon through the solutions for 30 min. Using a solution of

platinum octaethylporphyrin,²² this procedure resulted in phosphorescence lifetimes of >30 μs, which shows that the lifetimes measured for the tetracene derivatives were not limited by quenching due to residual O₂. Samples were prepared with a peak absorbance of less than 0.2 to prevent self-absorption effects.

Steady-state UV–vis absorption and fluorescence data were recorded using a Cary 50 Bio UV-Visible spectrometer and a Spex Fluorolog Tau-3 fluorescence spectrophotometer (excitation at 400 nm), respectively. Fluorescence quantum yields were determined in non-degassed solutions using anthracene in ethanol as standard.²³ Fluorescence lifetimes were taken by exciting the samples with 200 fs pulses centered at 400 nm. The pulses were generated using a 40 kHz regeneratively amplified Ti:Sapphire laser system and frequency doubling in a Type I BBO crystal. The fluorescence emission of room-temperature samples (no cryostat) was collected at 90° relative to the excitation, whereas for cooled samples the incident angle of the exciting laser beam was about 10° relative to the cuvette surface normal. The excitation pulses exhibited linear polarization, and the angle between the polarization of the collected fluorescence light and that of the excitation light was adjusted to 54.7° (magic angle), using a thin film polarizer, to eliminate time-dependent effects due to molecular reorientation. The fluorescence was directed into a monochromator attached to a picosecond streak camera (Hamamatsu C4334 Streakscope), which provides both time- and wavelength-resolved fluorescence data, with resolutions of 15 ps and 2.5 nm, respectively, and 80 000 sweeps were averaged for each sample.

Calculations. All quantum chemical calculations were performed with the Turbomole version 5.7 sets of programs.²⁴ The energy optimization of structures was performed at the B3LYP/SV(P) level of sophistication.²⁵ No symmetry constraints were applied during the optimization. The SV(P) basis set is considered as equivalent to the 6-31g(d) basis set in accuracy. For all calculations, a higher grid (*m* = 4) was employed. The electronic excitations were throughout obtained from the adiabatic approximation of time dependent density functional theory (TDDFT).²⁶

Results and Discussion

Arylene-linked bis(tetracenes) **1–3** were synthesized in two steps: bromination of tetracene to 5-bromotetracene and Suzuki coupling of 5-bromotetracene with corresponding arylene diboronic acids (Scheme 1). The modern popular approach for the monobromination of polycyclic arenes uses NBS in DMF.²⁷ However, the low solubility of tetracene in DMF prevents direct application of this procedure. We used chloroform to obtain better solubility of the tetracene and a small amount of DMF for the NBS, which permitted the synthesis of 5-bromotetracene in high yield (90%). The Suzuki coupling of 5-bromotetracene with arylene diboronic acids using Pd(PPh₃)₄ as a catalyst formed the target compounds only in a low yield (~10%). Varying the reaction conditions did not improve the yield. The combination Pd₂(dba)₃ with DPEPHos (bis(2-(diphenylphosphino)phenyl)ether) as a ligand was described as an efficient catalyst for the Suzuki coupling of sterically hindered, ortho-disubstituted benzenes.²⁸ The application of this catalytic system

(22) Yang, J.; Cyr, P. W.; Wang, Y.; Soong, R.; Macdonald, P. M.; Chen, L.; Manners, I.; Winnik, M. A. *Photochem. Photobiol.* **2006**, *82*, 262–267.

(23) Melhuish, W. H. *J. Phys. Chem.* **1961**, *65*, 229–235.

(24) Ahlrichs, R.; Bär, M.; Häser, M.; Horn, H.; Kölmel, C. *Chem. Phys. Lett.* **1989**, *162*, 165–169.

(25) Schäfer, A.; Horn, H.; Ahlrichs, R. *J. Chem. Phys.* **1992**, *97*, 2571–2577.

(26) Bauernschmitt, R.; Ahlrichs, R. *Chem. Phys. Lett.* **1996**, *256*, 454–464.

(27) Mitchell, R. H.; Lai, Y. H.; Williams, R. V. *J. Org. Chem.* **1979**, *44*, 4733–4735.

(28) Yin, J.; Rainka, M. P.; Zhang, X. X.; Buchwald, S. L. *J. Am. Chem. Soc.* **2002**, *124*, 1162–1163.

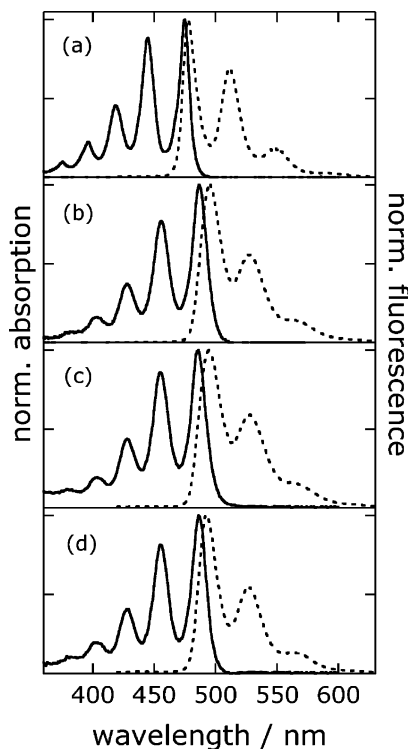


Figure 1. Normalized absorption (solid lines) and steady-state fluorescence (dashed lines) spectra of (a) tetracene, (b) **1**, (c) **2**, and (d) **3** in toluene.

to the coupling of 5-bromotetracene with arylene diboronic acid gave arylene-linked bis(tetracenes) **1–3** in 42–67% yield. Aqueous potassium carbonate was used instead of potassium phosphate in the original procedure to improve the yields of bis(tetracenes).

The steady-state absorption and fluorescence spectra for monomeric tetracene and molecules **1–3** are shown in Figure 1. The spectra of all four molecules are remarkably similar. The only differences are a slight red-shift and broadening of the dimer spectra. One additional difference is that the high-frequency vibronic progression in all three dimers is slightly less pronounced than in monomeric tetracene. From Figure 1, the ratio of the height of the 0–1 peak to the 0–0 peak in the tetracene emission spectrum is about 0.70, whereas in the dimers it is about 0.55. A similar decrease in the relative 0–1 intensity is also seen in the absorption spectra. The red-shift, broadening and change in vibronic intensities are all consistent with what has been observed for phenyl-substituted polyacenes.^{29–31} The spectral red-shift can be understood in terms of a slight increase in electronic delocalization due to the conjugated phenylene linker. The spectral broadening may be due to conformational disorder in the dimers, where different conformers have slightly different transition energies, or it may be that there are additional low-frequency vibrational modes coupled to the electronic transition in the dimers. The spectra are fairly insensitive to changes in solvent, shifting only a few nanometers as the solvent polarity is varied from toluene to CH_2Cl_2 to DMF. The lack of a pronounced solvatochromic effect in the dimer reveals the absence of significant through-bond charge transfer interactions.

(29) Jones, R. N. *Chem. Rev.* **1947**, *41*, 353–371.

(30) Zweig, A.; Gallivan, J. B. *J. Am. Chem. Soc.* **1969**, *91*, 260–264.

(31) Burgdorff, C.; Kircher, T.; Löhmansröben, H. G. *Spectrochim. Acta A* **1988**, *44*, 1137–1141.

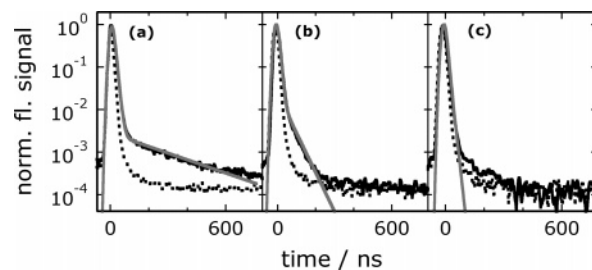


Figure 2. Time-resolved fluorescence decays of (a) **1**, (b) **2**, and (c) **3** in degassed (solid black lines) and oxygenated (dashed lines) toluene at room temperature. Also shown are fits to the data in degassed toluene with a function that contains the measured Gaussian instrument response convoluted with a biexponential decay (a and b) or a monoexponential decay (c) (solid gray lines).

This is in contrast to the widely studied bianthryl molecule, where in nonpolar solvents there is measurable excitonic coupling and in polar solvents a low-energy charge transfer state dominates the fluorescence.^{32–34} The presence of an extra phenyl group in the linkage between the tetracenes is apparently sufficient to prevent the strong electronic interactions seen in bianthryl, where the anthracene moieties are separated by only a single bond. We attempted to synthesize the single bond linked tetracene analog of bianthryl, but problems with purification and a lack of photostability prevented us from making reliable measurements on this molecule.

Although the steady-state spectroscopy clearly indicates that our bis(tetracene) derivatives **1–3** can be thought of as pairs of weakly coupled tetracene molecules, it provides no information about possible fission dynamics. Delayed fluorescence, resulting from intramolecular triplet recombination or “fusion”, provides an indirect way to monitor triplet dynamics and has been used extensively to characterize exciton fission in solid tetracene.^{35–38} The room-temperature fluorescence decays of derivatives **1–3** are shown in Figure 2 for both ambient and degassed toluene solutions. In compounds **1** and **2**, a clear biexponential decay appears in the degassed solutions. In both cases, the long-time component decays on a time scale of more than 100 ns, much longer than the radiative lifetime of either molecule (20–30 ns). Furthermore, the spectrum of this long-lived component is identical to that of the initial singlet emission, as shown in Figure 3. Note that the 500 nm peak in these spectra is diminished relative to that in the steady-state spectra in Figure 1. This is because the wavelength response of the streak camera detection setup was not uniform across the spectrum due to the use of spectral cutoff filters. This long-lived emission was observed in all solvents, regardless of polarity. The long-lived emission from molecules **1** and **2** must be due to the temporary storage of the singlet energy in a long-lived dark state where leakage back into the singlet state is allowed. The fact that the long-lived decay disappears when oxygen is present provides proof that it is not an artifact of the instrument response of our

(32) Fritz, R.; Rettig, W.; Nishiyama, K.; Okada, T.; Müller, U.; Müllen, K. *J. Phys. Chem. A* **1997**, *101*, 2796–2802.

(33) Nishiyama, K.; Honda, T.; Reis, H.; Müller, U.; Müllen, K.; Baumann, W.; Okada, T. *J. Phys. Chem. A* **1998**, *102*, 2934–2943.

(34) Grabner, G.; Rechthaler, K.; Köhler, G. *J. Phys. Chem. A* **1998**, *102*, 689–696.

(35) Ern, V.; Saint-Clair, J. L.; Schott, M.; Delacote, G. *Chem. Phys. Lett.* **1971**, *10*, 287–290.

(36) Arnold, S.; Alfano, R. R.; Pope, M.; Yu, W.; Ho, P.; Selsby, R.; Tharrats, J.; Swenberg, C. E. *J. Chem. Phys.* **1976**, *64*, 5104–5114.

(37) Arnold, S.; Whitten, W. B. *J. Chem. Phys.* **1981**, *75*, 1166–1169.

(38) Klein, G. *Chem. Phys. Lett.* **1978**, *57*, 202–206.

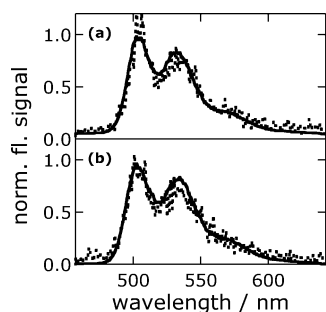


Figure 3. Fluorescence emission spectra of (a) **1** and (b) **2** in degassed toluene in the 0–70 ns time window (solid lines) and the 200–700 ns time window or the 80–270 ns time window (dotted lines) for **1** or **2**, respectively.

streak camera. Although O_2 is an effective triplet quencher, the fact that it quenches the long-lived fluorescence component is not proof that this component is due to a triplet state. In the case of tetracene, O_2 actually quenches the singlet state more efficiently than the triplet state.³⁹ Our assignment of the stored energy to a triplet pair state is based on known energy levels of tetracene and our calculated electronic structures. The absence of any long time component in monomeric tetracene is expected, since no triplet pair state is possible in this case. The steady-state spectroscopic data and prompt fluorescence decay times for all the molecules are summarized in Table 1. The most notable fact is that the phenyl substitution decreases the radiative lifetime, consistent with some electronic delocalization that enhances the transition dipole moment.

To analyze the bis(tetracene) dynamics measured in our time-resolved spectroscopy experiments, we utilize the model outlined in Figure 4. This model is the simplest one that captures the essential physics of the fission process.^{40,41} The populations of the S_1 , T_1 and $2T_1$ (triplet pair) states are determined by a set of three coupled linear differential equations:²⁰

$$\frac{\partial N_{S_1}}{\partial t} = -(k_{isc} + k_{ic} + k_{rad} + k_{fiss})N_{S_1} + k_{fus}N_{2T_1} \quad (3)$$

$$\frac{\partial N_{T_1}}{\partial t} = -k_{trip}N_{T_1} + k_{isc}N_{S_1} \quad (4)$$

$$\frac{\partial N_{2T_1}}{\partial t} = -(k_{trip} + k_{fus})N_{2T_1} + k_{fiss}N_{S_1} \quad (5)$$

In this system of equations, N_{S_1} , N_{T_1} , and N_{2T_1} are the populations of the excited singlet state, single triplet state per molecule, and triplet pair state, respectively; k_{isc} is the intersystem crossing rate, k_{ic} is the internal conversion rate, k_{rad} is the radiative decay rate, k_{trip} is the triplet decay rate, and k_{fiss} and k_{fus} are the fission and fusion rates, respectively. Note that since we only observe fluorescence, the effect of internal conversion on the fluorescence dynamics is indistinguishable from that of intersystem crossing. This set of equations can be quickly solved by matrix diagonalization using a standard package in an analysis program like MATLAB. In practice, $k_{fl} = k_{rad} + k_{isc} + k_{ic}$ is fixed by

(39) Murov, S. L.; Carmichael, I.; Hug, G. L. *Handbook of Photochemistry*, 2nd ed.; Marcel Dekker, Inc.: New York, 1993.

(40) Pope, M.; Geacintov, N. E.; Vogel, F. *Mol. Cryst. Liq. Cryst.* **1969**, *6*, 83–104.

(41) Swenberg, C. E.; Ratner, M. A.; Geacintov, N. E. *J. Chem. Phys.* **1974**, *60*, 2152–2157.

Table 1. Room-Temperature Energies of the Lowest Energy Absorption and Highest Energy Fluorescence Bands, Prompt Fluorescence Lifetimes, Quantum Yields, and Radiative Lifetimes of Tetracene and the Three Bis(tetracene) Molecules **1**, **2**, and **3** in Non-Degassed Benzene or Toluene Solution

molecule	tetracene	1	2	3
abs. band/cm ⁻¹	21 050	20 555	20 575	20 575
fl. band/cm ⁻¹	20 942	20 161	20 222	20 263
τ_{fl}/ns	3.88 ± 0.01	6.13 ± 0.02	5.44 ± 0.01	6.13 ± 0.02
Φ_{fl}	0.17 ± 0.02	0.31 ± 0.01	0.42 ± 0.02	0.35 ± 0.03
	(in benzene)	(in benzene)	(in toluene)	(in toluene)
τ_{rad}/ns	23 ± 3	19.8 ± 0.4	12.9 ± 0.7	17 ± 1

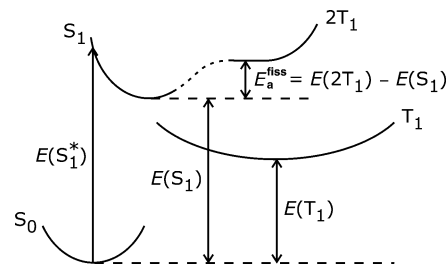


Figure 4. Energy level model for tetracene and the bis(tetracenes) **1**, **2**, and **3**.

the measured fluorescence decay time, whereas k_{rad} and $k_{ic} + k_{isc}$ are obtained from the measured fluorescence quantum yield Φ_{fl} in solution via the relation

$$\Phi_{fl} = \frac{k_{rad}}{k_{fl}} \quad (6)$$

Since the triplet lifetime of monomeric tetracene is $>600 \mu s$,^{39,42} we set $k_{trip} = 1 \text{ ms}$ when we simulate the data. At room temperature, tetracene in degassed solution has nonradiative rates $k_{ic} = 4.6 \times 10^7 \text{ s}^{-1}$ and $k_{isc} = 13 \times 10^7 \text{ s}^{-1}$,⁴² whereas we found a total nonradiative rate $k_{ic} + k_{isc} = 4.5 \times 10^7 \text{ s}^{-1}$ for **1** and **2** at room temperature. Substituted tetracenes like rubrene have been shown to have much higher fluorescence quantum yields than tetracene, so the reduced nonradiative rate in our substituted tetracenes is not too surprising. With these values, there are only two undetermined parameters in our model, namely k_{fiss} and k_{fus} . The relative magnitude of k_{fiss} compared to k_{fl} determines the point at which the initial rapid fluorescence decay changes over to a second exponential decay. This longer, delayed fluorescence component then decays with the lifetime of the triplet pair state, $2T_1$, which is determined by k_{fus} since k_{trip} is negligible on this time scale. By systematically varying these two rates so that the simulated data matches the experimental data, we determine k_{fiss} and k_{fus} , the remaining parameters in the scheme in Figure 4. Since very different parts of the data are sensitive to the different rate constants, we can be sure that the combination of k_{fiss} and k_{fus} obtained using this approach is unique to within the experimental error. Simulations using eqs 3–5 for the room-temperature fluorescence decay data are overlaid with the data in Figure 2. These simulations involve the convolution of the measured Gaussian instrument response with a biexponential decay that is obtained from solving eqs 3–5. Thanks to the high dynamic range of our streak camera measurements, we are able to obtain reliable estimates of both

(42) Burgdorff, C.; Ehrhardt, S.; Löhmansröben, H.-G. *J. Phys. Chem.* **1991**, *95*, 4246–4249.

Table 2. Room-Temperature Rates for Prompt Singlet Fluorescence (k_{rad}), Intersystem Crossing and Internal Conversion ($k_{\text{isc}}+k_{\text{ic}}$), Phosphorescence (k_{trip}), Exciton Fission (k_{fiss}) and Fusion (k_{fus}), Fission Activation Energies (E_a^{fiss}), Arrhenius Prefactors (A) for Fission and Fusion, and Fission Yields (Φ_{fiss}) of Molecules **1** and **2** in Degassed Toluene Solution

molecule	1	2
k_{rad}/s^{-1}	$(5.00 \pm 0.05) \times 10^7$	$(7.70 \pm 0.05) \times 10^7$
$(k_{\text{isc}} + k_{\text{ic}})/s^{-1}$	$(4.50 \pm 0.05) \times 10^7$	$(4.50 \pm 0.05) \times 10^7$
k_{trip}/s^{-1}	1×10^3	1×10^3
k_{fiss}/s^{-1}	$(2.8 \pm 0.2) \times 10^6$	$(4.0 \pm 0.2) \times 10^6$
k_{fus}/s^{-1}	$(3.0 \pm 0.2) \times 10^6$	$(10 \pm 1) \times 10^6$
$E_a^{\text{fiss}}/\text{cm}^{-1}$	840 ± 50	340 ± 40
A_{fiss}/s^{-1}	$(1.48 \pm 0.04) \times 10^8$	$(1.72 \pm 0.02) \times 10^7$
A_{fus}/s^{-1}	$(3.20 \pm 0.02) \times 10^6$	$(8.9 \pm 0.1) \times 10^6$
$A_{\text{fiss}}/A_{\text{fus}}$	46 ± 1	1.94 ± 0.04
Φ_{fiss}	0.028 ± 0.002	0.029 ± 0.001

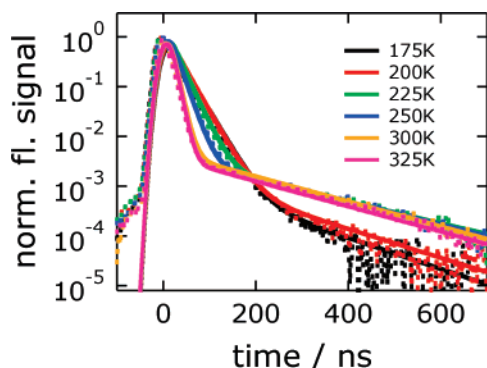


Figure 5. Time-resolved fluorescence decays of **1** in degassed solvent mixture (toluene/isopentane/DMF 3:3:2) as a function of temperature (dotted lines). Also shown are fits to the data with a function that contains the measured Gaussian instrument response convoluted with a biexponential decay (solid lines).

parameters even when small k_{fiss} values lead to low fission yields Φ_{fiss} , defined as

$$\Phi_{\text{fiss}} = \frac{k_{\text{fiss}}}{k_{\text{f}} + k_{\text{fiss}}} \quad (7)$$

Φ_{fiss} is on the order of 2–3% for molecules **1** and **2**, with no measurable fission yield in **3**. The kinetic parameters used to fit the data are summarized in Table 2. Note that these parameters have been used to fit the data for the degassed samples in the cryostat and yield a quantum yield of 0.49 for **1**. When adjusted for O_2 singlet quenching,³⁹ the quantum yield falls to 0.32, consistent with the non-degassed sample data in Table 1.

Given a model that allows us to extract k_{fiss} and k_{fus} from the experimental data, we can now look at these rates as a function of temperature to extract information about the energetics of the fission and fusion reactions. In Figure 5, we show the temperature dependence of the fluorescence decay of molecule **1** in a toluene/DMF/isopentane solvent mixture that is formulated to remain a liquid down to 150 K. Both the short-time decay component and the amplitude of the long-time component change over the temperature range 175–325 K, whereas the decay time of the long component remains essentially constant. Below 175 K, the long-time decay was so diminished that it could no longer be reliably distinguished from the background noise. Using the model outlined in Figure 4, we can determine both k_{fiss} and k_{fus} as a function of temperature. Arrhenius plots

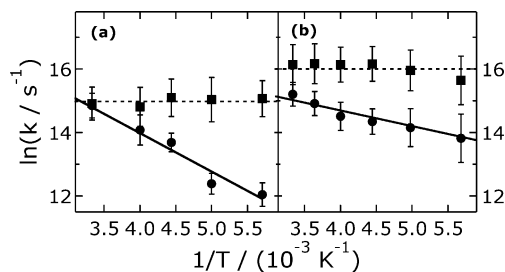


Figure 6. Temperature dependence of fission (●) and fusion (■) rates of (a) **1** and (b) **2**. Also shown are linear fits to the fission (solid lines) and fusion (dashed lines) rates.

of this data for compounds **1** and **2** are given in Figure 6a and b. In both compounds, the $\ln(k_{\text{fiss}})$ data undergoes a linear decrease with $1/T$, yielding activation energies of $840 \pm 50 \text{ cm}^{-1}$ ($10.0 \pm 0.6 \text{ kJ/mol}$) for **1** and $340 \pm 40 \text{ cm}^{-1}$ ($4.1 \pm 0.5 \text{ kJ/mol}$) for **2**. The k_{fus} data, on the other hand, exhibit almost no temperature dependence, suggesting a negligible barrier for the reverse reaction in both molecules. This observation is consistent with the energy level model in Figure 4. The Arrhenius prefactors can be obtained from the data in Figure 6 as well. The fission prefactors differ by almost 1 order of magnitude, $1.5 \times 10^8 \text{ s}^{-1}$ for **1** and $1.7 \times 10^7 \text{ s}^{-1}$ for **2**. This difference in prefactor values may be due to weaker electronic coupling between the tetracene moieties in **2**, as discussed below. For the fusion reaction, the Arrhenius prefactors are $(3 \pm 1) \times 10^6 \text{ s}^{-1}$ for **1** and $(8 \pm 3) \times 10^6 \text{ s}^{-1}$ for **2**. The values are almost identical to within the range of experimental error. When fitting the temperature-dependent data, we also obtain values for the $k_{\text{isc}}+k_{\text{ic}}$ nonradiative decay rate ranging from $6.2 \times 10^7 \text{ s}^{-1}$ to $1.0 \times 10^5 \text{ s}^{-1}$. By plotting this rate versus $1/T$ from 325 to 250 K, an estimate of the activation energy for the nonradiative relaxation pathway of approximately 2000 cm^{-1} is obtained for both **1** and **2**. This value is consistent with values obtained for phenyl-substituted tetracene derivatives.^{31,43}

Our experimental results show that the bis(tetracene) derivatives **1** and **2** undergo thermally activated exciton fission, but with low yields. Molecule **3**, on the other hand, shows no discernible signs of fission. To gain further insight into the origins of the different behaviors seen in molecules **1–3**, we turned to *ab initio* calculations to address three main questions. The first concerns the conformation of the dimers—what are the orientations of the tetracene rings with respect to the linker and can they rotate freely in solution? The second question concerns the energy levels in the compounds. Can the differences in E_a for **1** and **2**, or the lack of fission in **3**, be understood in terms of shifting energy levels? In the simple model outlined in Figure 4, the activation energy $E_a^{\text{fiss}} = E(2T_1) - E(S_1)$ can be deduced from the calculated S_1 and T_1 energies. Finally, is there any indication that electronic coupling in the singlet excited-state manifold plays a role in determining the size of the Arrhenius prefactors in the fission and fusion rates?

Figure 7a–c shows the energy minimized ground state (S_0) structures for **1–3**. In all three molecules, the linker phenyl groups are rotated by ~ 90 degrees relative to the tetracene moieties due to steric interactions. The lack of planar π -electron pathways would be expected to prevent efficient through-bond electron delocalization and explains why the spectroscopy of

(43) Komfort, M.; Löhmansröben, H.-G.; Salthammer, T. *J. Photochem. Photobiol. A* **1990**, *51*, 215–227.

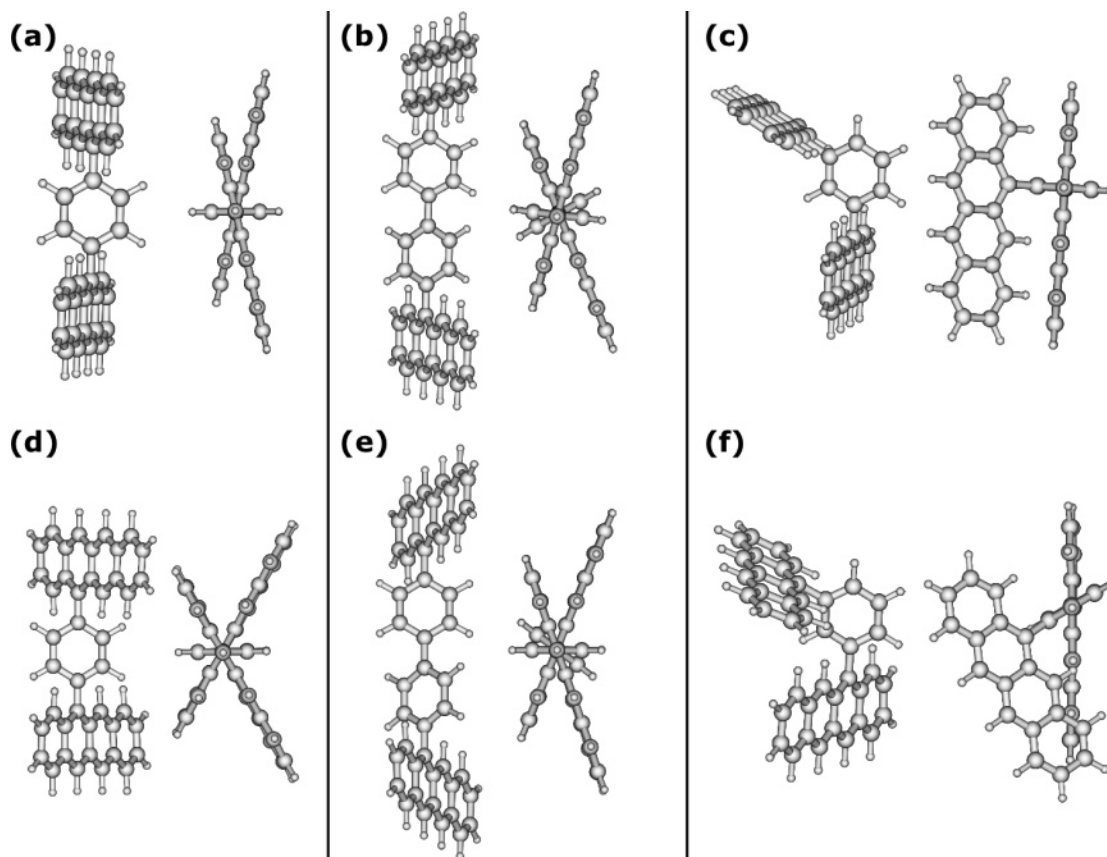


Figure 7. Geometry optimized singlet ground state (a–c) and relaxed first excited singlet state (d–f) structures (left: side view, right: top view) of **1** (a,d), **2** (b,e), and **3** (c,f).

the dimers is so similar to that of the monomer. Calculations on different conformers allow us to estimate a barrier for rotation for the tetracene rings in **1** to be ~ 4 – 8 kJ/mol, comparable to kT at room temperature. This is similar to the rotational barrier in biphenyl, which has a similar bonding situation and has been a topic of intensive investigation.⁴⁴ The calculated barrier for rotation in this molecule is rather small, and for the planar conformation, the (repulsive) eclipsed hydrogen–hydrogen interactions are counteracted by (attractive) dispersive interactions, which in general are not properly accounted for by density functional calculations. This leads to some uncertainty in the absolute value of the barrier, but probably not more than 4 kJ/mol. So it is likely that these molecules rotate easily in solution and are not locked into a single conformation. Slight energy differences between rotamers would provide a qualitative explanation for the broadened absorption and fluorescence spectra seen for the dimers in Figure 1.

The second question is whether energy level shifts in the dimer molecules can help explain the different observed fission and fusion rates. Analysis of the data in Figure 6 suggests that the fission activation energy E_a^{fiss} in **2** is about 50% of that in **1**. According to Figure 4, this could come about if the $S_1 \rightarrow 2T_1$ energy gap in **2** is lower than in **1**. The calculation of excited-state energies is less straightforward than that of ground state properties, but our hybrid TDDFT method produced good agreement with experimental transition energies, which was encouraging. We first examined the $S_0 \rightarrow S_1^*$ absorption

energies of tetracene and its phenylene-substituted derivatives listed in Table 3. In tetracene, the experimental 0–0 absorption peak is located at $21\,050\text{ cm}^{-1}$, whereas the calculated energy of the vertical transition is $19\,822\text{ cm}^{-1}$, a shift of about 1200 cm^{-1} or about 0.15 eV . This is well within the typical accuracy expected for TDDFT calculations,⁴⁵ and we did not attempt to scale the calculated energies to obtain better agreement with experiment. The calculated triplet energy is also slightly lower than the experimental value for tetracene.^{39,46,47} The addition of phenylene linkers to the 5-position of tetracene leads to a small shift to lower energy for both the singlet and triplet states. The singlet states are lowered in energy by about 300 cm^{-1} by the first phenylene group. Similarly, the first phenylene group appears to lower the triplet energy by 200 cm^{-1} . For both singlet and triplet states, these results are consistent with experimental data for phenyl-substituted polyacenes, where the excited-state energies are typically lowered by a few hundred cm^{-1} .^{30,31} Subsequent additions to the linker have little effect on the energies, with shifts of at most 100 cm^{-1} . For all the single tetracene molecules, the calculations yield only a single state in the correct energy range and it is straightforward to identify the strongly allowed singlet and triplet states that correspond to the experimentally observed states.

The situation becomes more complicated when the linker is terminated by a second tetracene. The second tetracene has a

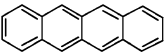
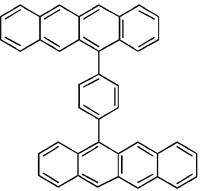
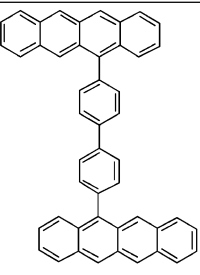
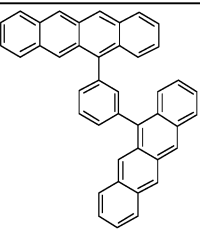
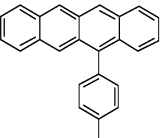
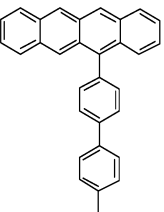
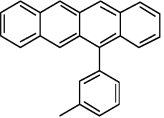
(44) Tsuzuki, S.; Uchamaru, T.; Matsumura, K.; Mikami, M.; Tanabe, K. *J. Chem. Phys.* **1999**, *110*, 2858–2861.

(45) Dreuw, A.; Head-Gordon, M. *Chem. Rev.* **2005**, *105*, 4009–4037.

(46) Volcker, A.; Adick, H. J.; Schmidt, R.; Brauer, H. D. *Chem. Phys. Lett.* **1989**, *159*, 103–108.

(47) McGlynn, S. P.; Azumi, T.; Kasha, M. *J. Chem. Phys.* **1964**, *40*, 507–515.

Table 3. Calculated Energies and Mixed Representations for Oscillator Strengths of the Transitions from the Relaxed S_0 State to the Unrelaxed S_1^* State of Tetracene, the Bis(tetracenes) **1**, **2**, and **3**, and Three Single Tetracene Molecules with Methyl-Terminated Linker Groups^a

molecule	$E(S_1^*) / \text{cm}^{-1}$	osc. strength
	19,822*	0.0634
 1	19,109* 19,589	0.141 0.0804
 2	19,417*	0.238
 3	18,857* 19,616	0.0710 0.0910
	19,516	0.0920
	19,497	0.110
	19,539	0.0894

^a The lowest energy state with appreciable oscillator strength that is considered in further calculations is marked with an asterisk.

negligible effect on the triplet state energy and does not result in the appearance of extra allowed states in the calculations. The insensitivity of the triplet energies to linker structure or even to the presence of a second tetracene suggests that the triplet state is localized on one side of the dimer. This is consistent with the small triplet exciton bandwidths seen in polyacene molecular crystals^{48,49} and supports our hypothesis

that two triplet states can exist independently on the two tetracene moieties. The situation is different for the singlet states, which shift and split into multiple lines with the addition of the second tetracene. This behavior is due to excitonic interactions, similar to what is seen in “super molecule” calculations on dimers,^{50,51} where TDDFT has been successfully applied.⁵² These excitonic interactions will be discussed in more detail below. For now, we simply point out that the results of the bis-(tetracene) calculations require us to make two choices to estimate E_a^{fiss} . First, given the multiplicity of states generated by the calculations, we must choose which one to use for calculating the relevant energy differences. Since the triplet states appear unaffected by the excitonic interactions, the energy of the $2T_1$ state is just taken to be $E(2T_1) = 2 \times E(T_1)$. For the S_1 state, we take the lowest energy state with appreciable oscillator strength. This state is indicated for molecules **1–3** in Table 3. The second question concerns the geometry to be used for the calculation of the energy differences. Optical absorption induces an instantaneous transition from the relaxed S_0 state to the unrelaxed S_1^* state, as shown in Figure 4. Since the exciton fission rate is much slower than the vibrational relaxation rate, it is safe to assume that fission occurs from the relaxed S_1 geometry and not from the S_1^* geometry. Experimentally, we have found that there is no activation energy for the fusion reaction, which suggests that the energy at the top of the barrier is the same as that of the relaxed T_1 state. So the appropriate energy difference $2E(T_1) - E(S_1)$ should be taken at two different geometries, the relaxed S_1 and the relaxed T_1 , both of which are distinct from the relaxed S_0 state from which absorption first occurs. This situation is illustrated schematically in Figure 4 and the relevant energy parameters from the calculations are summarized in Table 4.

When these different energies are evaluated, we find that the trend in energies qualitatively follows the experimental results. When the energy difference $E_a^{\text{fiss}} = E(2T_1) - E(S_1)$ is evaluated for molecules **1–3**, we find that molecule **1** has a larger E_a^{fiss} than **2**, 851 cm^{-1} as opposed to 715 cm^{-1} . This is in qualitative agreement with the trend in experimentally measured E_a^{fiss} values, 840 cm^{-1} and 340 cm^{-1} for **1** and **2**, respectively. We were unable to detect any delayed fluorescence for **3**, and the E_a^{fiss} values in Table 4 provide one possible explanation. **3** has a calculated $E_a^{\text{fiss}} = 1675 \text{ cm}^{-1}$, more than twice that of **1** and **2**. Even given the same Arrhenius prefactor, this increase in the activation energy would be enough to decrease the fission rate by a factor of 100, effectively making it undetectable. The origin of the increased E_a^{fiss} in **3** appears to lie mostly with the extra energy difference between the unrelaxed S_1^* state accessed by photon absorption and the fully relaxed S_1 state where fission occurs. All three bis(tetracene) molecules in the relaxed S_1 state undergo significant geometrical distortions as shown in Figure 7d–f, with **1** and **3** showing the greatest changes from the initial $S_0(S_1^*)$ geometries in Figure 7a–c. Since the energy of the triplet state is insensitive to the presence of a second tetracene and the structural details of the phenylene linker, these excited-

- (48) Robinson, G. W. *Ann. Rev. Phys. Chem.* **1970**, *21*, 429–474.
 (49) Hochstrasser, R. M.; Li, T. Y.; Sung, H. N.; Wessel, J.; Zewail, A. H. *Pure. Appl. Chem.* **1974**, *37*, 85–96.
 (50) Bazan, G.; Oldham, W. J.; Lachicotte, R. J.; Tretiak, S.; Chernyak, V.; Mukamel, S. *J. Am. Chem. Soc.* **1998**, *120*, 9188–9204.
 (51) Beljonne, D.; Cornil, J.; Silbey, R.; Millie, P.; Bredas, J. L. *J. Chem. Phys.* **2000**, *112*, 4749–4758.
 (52) Clark, A. E.; Qin, C.; Li, A. D. Q. *J. Am. Chem. Soc.* **2007**, *129*, 7586–7595.

Table 4. Calculated Energies of the Relaxed First Excited Singlet State (S_1), Relaxed First Excited Triplet State (T_1), Calculated Energy Differences between the Unrelaxed and the Relaxed First Excited Singlet State ($E(S_1^*) - E(S_1)$), and Calculated Activation Energy for Fission (E_a^{fiss}) of Tetracene and the Bis(tetracenes) **1**, **2**, and **3** (see State Diagram in Figure 4)

molecule	$E(S_1)/\text{cm}^{-1}$	$E(T_1)/\text{cm}^{-1}$	$E(S_1^*) - E(S_1)/\text{cm}^{-1}$	$E_a^{\text{fiss}} = E(2T_1) - E(S_1) / \text{cm}^{-1}$
tetracene	18 478	9 534	1 344	590
1	17 821	9 336	1 288	851
2	17 967	9 341	1 450	715
3	16 945	9 310	1 912	1 675

state geometry changes appear to be the primary factors determining E_a^{fiss} . It should also be pointed out that the choice of molecular geometry plays an important role in the estimation of the activation energies. If we had used the unrelaxed S_1^* energies in Table 3 to predict trends in the activation energies, we would have obtained negative E_a^{fiss} values for all three molecules, as well as a smaller E_a^{fiss} value for **1** relative to **2**, the opposite of what is observed experimentally. Finally, we should note that all the energy differences discussed here are comparable to or less than the amount of absolute error ($\sim 1200 \text{ cm}^{-1}$) in the energies calculated using our TDDFT method. Thus, the numerical values for the energies should not be taken too seriously. The important point is that the calculations provide a qualitative way to explain the observed experimental trends and highlight some subtleties of the energetic factors involved.

A final question we tried to address using the calculations was the role of interchromophore electronic coupling in determining the fission rate, presumably by affecting the Arrhenius prefactors. Some workers have speculated that the presence of singlet–singlet electronic interactions, accompanied by the presence of delocalized intermolecular exciton states, might enhance the singlet fission rate.⁵³ We begin with a discussion of the nature of the electronic coupling between the two tetracenes. Electronic coupling in the bis(tetracene) molecules can be of two types: through-space Coulomb coupling, and through-bond electron-transfer coupling.^{54–56} We can estimate the magnitude of the through-space term by assuming a point-dipole interaction between the two tetracene transition dipole moments:^{56,57}

$$V_{12} = \frac{|M|^2}{4\pi\epsilon r_{12}^2} (\cos \alpha + 3 \cos^2 \theta) \quad (8)$$

In this expression, M is the transition dipole moment ($0.82 \times 10^{-29} \text{ C m}$ for tetracene),^{58,59} r_{12} is the center-to-center distance between the transition dipoles, which are assumed to be exactly centered in the tetracene rings and oriented perpendicular to the long molecular axis. ϵ is the dielectric constant of the medium ($\epsilon = 2.38\epsilon_0$ for toluene), with $4\pi\epsilon_0$ taken to be $1.11265 \times 10^{-10} \text{ C}^2\text{s}^2\text{kg}^{-1}\text{m}^{-3}$. α is the angle between the dipoles, and θ is the angle made by the dipole with the center-to-center line. For molecule **1**, where the tetracene rings are rotated 180° with respect to each other, similar to what is seen in Figure 7, we

obtain an interaction energy $V_{12} = 85 \text{ cm}^{-1}$. Since the point dipole method tends to overestimate the V_{12} interaction term, this value should be taken as an upper bound for V_{12} .^{60–64} The splitting of the absorption is given by $2V_{12} = 170 \text{ cm}^{-1}$, corresponding to about 4 nm in this wavelength range, which is less than the observed line broadening. We can similarly estimate $V_{12} = 25 \text{ cm}^{-1}$ in **2** and $V_{12} = 90 \text{ cm}^{-1}$ in **3**. These analytical calculations can be compared to the results of *ab initio* calculations given in Table 3. These calculations predict that tetracene and **2** both have only a single, strongly allowed singlet absorption at energies of $19 822 \text{ cm}^{-1}$ and $19 417 \text{ cm}^{-1}$, respectively. But for molecules **1** and **3**, where the tetracene rings are separated by only a single phenylene group, the calculations predict a pair of strongly allowed absorption peaks located at $19 109 \text{ cm}^{-1}$ and $19 589 \text{ cm}^{-1}$ for **1** and $18 857 \text{ cm}^{-1}$ and $19 616 \text{ cm}^{-1}$ for **3**, leading to estimates of $V_{12} = 240 \text{ cm}^{-1}$ for **1** and $V_{12} = 380 \text{ cm}^{-1}$ for **3**. The small V_{12} values obtained from the “optimistic” through-space calculations using eq 8 suggest that the larger calculated V_{12} values are due to through-bond interactions. For example, when the spectra of the conformers in Figure 7 are recalculated after removal of the linker phenyl, so the through-bond mechanism is no longer operative, the splitting disappears and the two lines are replaced by a single absorption at $\sim 20 000 \text{ cm}^{-1}$. Furthermore, the calculated spectra for different phenylene conformers gives rise to different splittings, and when the linker phenyl group is twisted perpendicular to the tetracene rings, the splitting is minimized. The physical origin of the splittings in the calculations can thus be assigned to through-bond interactions, but the question remains as to why these splittings are not seen experimentally. One likely explanation is the conformational flexibility present in all three molecules. Electronic delocalization in biphenyl has been shown to be very sensitive to the torsion angle between the phenyl rings,⁶⁵ and it is likely that electronic communication through the bis(tetracene) molecules can also be disrupted by changes in twist angles. Facile rotation of the tetracene rings would give rise to a distribution of interaction energies, and this distribution may be at least partially responsible for the broadened lineshapes in Figure 1. For these reasons, it is probably impossible to make quantitative statements about the relative magnitudes of V_{12} without performing a thermal average over all possible conformations in the relaxed S_1 state. What we can say is that the through-bond interactions appear to be much larger than the through-space couplings, and

(53) Swenberg, C. E.; Geacintov, N. E., Eds. *Excitonic interactions in organic solids*; Wiley & Sons: Bristol, 1973; Vol. 1, pp 489–564.

(54) Harcourt, R. D.; Scholes, G. D.; Ghiggino, K. P. *J. Chem. Phys.* **1994**, *101*, 10521–10525.

(55) Scholes, G. D.; Harcourt, R. D.; Ghiggino, K. P. *J. Chem. Phys.* **1995**, *102*, 9574–9581.

(56) Thompson, A. L.; Gaab, K. M.; Xu, J.; Bardeen, C. J.; Martinez, T. J. *J. Phys. Chem. A* **2004**, *108*, 671–682.

(57) Kasha, M.; Rawls, H. R.; El-Bayoumi, M. A. *Pure. Appl. Chem.* **1965**, *11*, 371–392.

(58) Kleven, H. B.; Platt, J. R. *J. Chem. Phys.* **1949**, *17*, 470–481.

(59) Tanaka, J. *Bull. Chem. Soc. Jap.* **1965**, *38*, 86–103.

(60) Czikkely, V.; Försterling, H. D.; Kuhn, H. *Chem. Phys. Lett.* **1970**, *6*, 207–210.

(61) Krueger, B. P.; Scholes, G. D.; Fleming, G. R. *J. Phys. Chem. B* **1998**, *102*, 5378–5386.

(62) Ortiz, W.; Krueger, B. P.; Kleiman, V. D.; Krause, J. L.; Roitberg, A. E. *J. Phys. Chem. B* **2005**, *109*, 11512–11519.

(63) Beenken, W. J. D.; Pullerits, T. *J. Chem. Phys.* **2004**, *120*, 2490–2495.

(64) Wong, K. F.; Bagchi, B.; Rosicky, P. J. *J. Phys. Chem. A* **2004**, *108*, 5752–5763.

(65) Wang, J.; Cooper, G.; Tulumello, D.; Hitchcock, A. P. *J. Phys. Chem. A* **2005**, *109*, 10886–10896.

would be expected to be the main contributors to the fission rate. Through-bond couplings that depend on conformation could provide transient opportunities for exciton fission, in much the same way that solvent and conformational fluctuations lead to transient electron-transfer events in bianthryl⁶⁶ and which control electron transfer in phenylene-bridged donor–acceptor molecules.⁶⁷ On average, the through-bond term in the meta-linked molecule **3** would be expected to be smaller than that in the para-linked dimers **1** and **2**. This expectation is not fulfilled by the large V_{12} calculated for **3**, but this in turn may be an artifact of comparing single conformations instead of sampling over all possible conformations. The longer linker in **2** is expected to have a weaker coupling than in **1**, and this trend is indeed seen in the calculations and also in the experimental values for the Arrhenius prefactors in Table 4.

The fission rates for **1** and **2** in Table 2 are much less than the literature values for k_{fiss} in solid tetracene, which range from 1.2×10^8 to $8 \times 10^9 \text{ s}^{-1}$.^{36–38,68,69} To improve the fission yield, one can imagine two approaches. The first is to improve the electronic coupling between the two tetracene moieties. Previously we speculated that the low fission yield in **1** was due to weak electronic coupling between the tetracene moieties.²⁰ Intermolecular coupling in the solid is relatively strong, as evidenced by the existence of a Davydov splitting ($2V_{12}$) in the absorption spectrum of $\sim 650 \text{ cm}^{-1}$.^{59,70} This strong coupling gives rise to delocalized singlet exciton states that extend over an average of 10 molecules in polycrystalline samples.¹⁷ Such delocalized excitonic states would be expected to have good spatial overlap with a doubly excited triplet state that spans two molecules.⁵³ To increase the tetracene–tetracene coupling in our covalent molecules, we could either shorten the linker, increasing the through-space interaction (as in the solid), or force the tetracenes to remain planar, increasing the through-bond interaction. As mentioned earlier, a single-bond variant was synthesized but was not sufficiently stable for reliable spectroscopic measurements. Calculations suggest that such a molecule would have the tetracenes rotated 90° with respect to each other, similar to the situation in bianthryl.³⁴ A more promising linker group would be an ethynyl bridge, which would provide enough space for the tetracene rings to remain planar as well as a more robust pathway for π -electron communication. Planarity could be enforced by either choosing a constrained solvent environment, or by attaching additional functional groups to the tetracene rings to prevent large rotational displacements. Of course, improving the through-bond coupling also carries the risk that electron transfer across the bridge will lead to a low-energy charge-transfer state as in bianthryl.^{33,34} In this case, the triplet pair state would not be the lowest relaxation energy pathway, and the strong coupling would lead to the disappearance of the fission channel altogether.

A second approach to increasing k_{fiss} is to make the fission process more energetically favorable. One problem with tetracene is that $E(2T_1)$ is very close to $E(S_1)$, and we have seen how changes in chemical structure can lower the S_1 energy

significantly in the meta-coupled bis(tetracene) **3**. By making the T_1 state lower in energy, the fission reaction can be downhill, which both provides an extra driving force and also prevent the loss of the triplet pair through recombination, which now becomes energetically unfavorable. Michl and co-workers have done an extensive study of different organic molecule types and have identified several motifs in which exciton fission would be energetically allowed.¹³ A simple example in the polyacene family is pentacene, with roughly the same Davydov splitting as tetracene^{71,72} but where $E(2T_1) - E(S_1)$ is estimated to be about -4000 cm^{-1} .³⁹ In solid films, the fission reaction is estimated to take place on the order of 100 fs,⁷³ as opposed to $\sim 150 \text{ ps}$ in solid tetracene. The only problem with the approach of lowering the triplet energy is that it leads to a loss of overall energy efficiency, since the excess energy left over after generating the triplet state pair is dissipated as heat and cannot contribute to the electrochemical potential energy of an electron–hole pair.

Although not central to this work, it is worth speculating on the fate of the triplet pair state produced by exciton fission. Ideally, this state would be long-lived so that both states could be harvested and provide energy to produce two electron–hole pairs. In inorganic nanocrystals, exciton–exciton annihilation rapidly removes the fission products on the picosecond time scale.¹⁴ The decay of the delayed fluorescence in our bis-(tetracene) molecules suggests that the triplet pair can survive on the order of 100 ns in these compounds. We have so far assumed that the dominant decay channel is triplet fusion, $T_1 + T_1 \rightarrow S_1$. But in crystalline tetracene, the $T_1 + T_1 \rightarrow T_1^* \rightarrow T_1$ annihilation channel has been found to play a significant role as well.^{35,40} It should be noted that solid tetracene has the advantage that the triplet–triplet recombination yield is suppressed by the ability of the triplet excitons to rapidly diffuse away from each other into the bulk solid.⁷⁴ To accurately determine the relative importance of these two channels in the decay of the triplet pair, it is necessary to monitor both the S_1 and T_1 populations simultaneously, for example using frequency resolved transient absorption. Such an experiment is impractical for the current family of compounds due to the very low fission yields, but has been shown to be a valuable tool for detecting the possible role of fission in conjugated polyenes.^{75,76}

Conclusion

In this work, we have synthesized a series of bis(tetracene) molecules to investigate the phenomenon of intramolecular exciton fission. By characterizing the dynamics and temperature dependence of both the prompt and delayed singlet fluorescence, we have shown that para-phenylene linked molecules **1** and **2** show fission yields on the order of 2–3%, whereas the meta-linked molecule **3** shows no measurable fission. *Ab initio* calculations indicate that the molecules are conformationally flexible, which can mediate the interchromophore interactions

- (66) Piet, J. J.; Schuddeboom, W.; Wegewijs, B. R.; Grozema, F. C.; Warman, J. M. *J. Am. Chem. Soc.* **2001**, *123*, 5337–5347.
(67) Weiss, E. A.; Tauber, M. J.; Kelley, R. F.; Ahrens, M. J.; Ratner, M. A.; Wasielewski, M. R. *J. Am. Chem. Soc.* **2005**, *127*, 11842–11850.
(68) Groff, R. P.; Avakian, P.; Merrifield, R. E. *Phys. Rev. B* **1970**, *1*, 815–817.
(69) Fleming, G. R.; Millar, D. P.; Morris, G. C.; Morris, J. M.; Robinson, G. W. *Aust. J. Chem.* **1977**, *30*, 2353–2359.
(70) Philpott, M. R. *J. Chem. Phys.* **1969**, *50*, 5117–5128.

- (71) Schlosser, D. W.; Philpott, M. R. *Chem. Phys.* **1980**, *49*, 181–199.
(72) He, R.; Tassi, N. G.; Blanchet, G. B.; Pinczuk, A. *Appl. Phys. Lett.* **2005**, *87*, 103107/1–103107/3.
(73) Jundt, C.; Klein, G.; Sipp, B.; LeMoigne, J.; Joucla, M.; Villaeys, A. A. *Chem. Phys. Lett.* **1995**, *241*, 84–88.
(74) Aladekomo, J. B.; Arnold, S.; Pope, M. *Phys. Stat. Sol. B* **1977**, *80*, 333–340.
(75) Gradinaru, C. C.; Kennis, J. T. M.; Papagiannakis, E.; van Stokkum, I. H. M.; Cogdell, R. J.; Fleming, G. R.; Niederman, R. A.; van Grondelle, R. *Proc. Natl. Acad. Sci.* **2001**, *98*, 2364–2369.
(76) Tavan, P.; Schulten, K. *Phys. Rev. B* **1987**, *36*, 4337–4358.

and result in broadened lineshapes rather than clear exciton splittings. The calculations reproduce the trend in fission activation energies, which are largely determined by the energetics of the excited singlet state and in particular the position of the relaxed S_1 state. The lowering of S_1 is most pronounced in molecule **3** and provides a possible explanation for the lack of observed fission in this molecule. Finally, the electronic interaction between the tetracenes appears to be dominated by through-bond interactions, leading to both the sensitivity to conformation and to reduced coupling in **3** due to its meta-conjugated linker. Thus, we can qualitatively explain the relative trends in fission between molecules **1–3** based on the *ab initio* results and basic chemical principles. This is a promising first step, although a more detailed theoretical

understanding of the fission reaction will be necessary for the design of molecules that have exciton fission yields approaching the 50% level. At this threshold, it would be possible to achieve a total quantum yield greater than unity, making this phenomenon of practical interest for the design of organic solar cells.

Acknowledgment. C.J.B. acknowledges the support of the National Science Foundation, grant CHE-0517095.

Supporting Information Available: Calculations and Cartesian coordinates of optimized geometries. This material is available free of charge via the Internet at <http://pubs.acs.org>.

JA073173Y